Solid State Phenomena
ISSN: 1662-9779, Vol. 390, pp 207-220
doi:10.4028/p-NzE5Rj

Submitted: 2026-02-16
Revised: 2026-02-23
Accepted: 2026-02-24
Online: 2026-04-17

Modeling the Influence of Material Variabilities on the Forming and Failure Behavior of PP/PE Cores in Metal-Polymer-Metal Sandwich Sheets

Johannes Pusicha[1,a*] and Johannes Buhl[1,b]

[1]Institute of Metallurgy, Clausthal University of Technology, 38678 Clausthal-Zellerfeld, Germany

[a*]johannes.pusicha@tu-clausthal.de, [b]johannes.buhl@tu-clausthal.de

*corresponding author

Keywords: sandwich composites, material characterization, material inhomogeneity.

Abstract. Metal-polymer-metal (mpm) sandwich sheets are considered a lightweight alternative to conventional steel sheets in the automotive industry. First studies have experimentally and numerically demonstrated the use of mpm-sandwiches in automotive crash structures. However, the sandwich forming process can compromise the crash performance through pre-damage. Finite element simulations could help predict the forming process and its limits. Current simulation approaches, however, consider neither strain rate effects and failure of the polymer and the adhesive, respectively, nor do they study the influence of inevitable material variabilities on the forming and failure behavior. In this work, a detailed finite element model of the core materials is developed. An approach for the determination of the stress strain rate dependency is proposed by evaluating the local strains on the surface, which allows capturing the main material behavior with little effort. Additional specialized tensile tests and lap-shear tests provide information about the failure of the polymer and the adhesive, respectively. Validation of the core materials model is achieved by comparing the cover layer displacements of swivel bending specimens in experiment and simulation. The influence of material variabilities on the forming and failure behavior is studied in a full factorial material parameter sweep of simulated lap-shear tests, and the applicability of the model to the simulation of bending processes is demonstrated. The results prove the applicability of the proposed material characterization methods, while the parameter study and the bending simulations show how the model can be used to predict a sandwich's formability and failure modes.

Introduction

To reduce the energy consumption of automobiles, research interest in weight-saving materials and designs for the automotive industry continues to be high. Metal-polymer-metal (mpm) sandwich sheets are considered a lightweight alternative to conventional steel sheets with possible uses in the vehicle chassis [1] or skin [2]. Two metal sheets (cover sheets) are joined with a polymer foil by using an epoxy resin adhesive, which increases the stiffness of the composite compared to the individual materials by only adding minimal weight.

First studies have experimentally and numerically evaluated the use of mpm sandwiches in automotive crash structures [3], such as double- or top-hat crash boxes [4]. As in conventional crash structures, the energy is absorbed by performing plastic deformation through progressive fold formation [5]. The energy absorption of these structures, therefore, depends on the material's stiffness and strength. However, due to the composite nature of mpm sandwich sheets, the interface properties of the sandwich have a significant influence on the crash performance, as has been investigated for the adhesion strength [6], and as can be concluded for the polymer core from characterizing experiments [7]. However, sandwich sheets have to undergo a series of forming steps before their use as a crash absorber, which can lead to undesirable pre-damage. FEM (finite element method) simulations of the sandwich forming process could help to predict the influence of the manufacturing process on the final crash performance. Detailed modelling of the core materials' (adhesive and polymer foil) forming and failure behavior is therefore needed, which has not yet been incorporated in current simulation approaches [7]. Additionally, to predict formability limits of sandwich sheets,

the influence of inevitable material and adhesion variabilities on the forming and failure behavior needs to be studied.

Therefore, in the following, a detailed FE model considering strain rate effects and failure of the core materials of mpm sandwich sheets is developed. In addition, since significant variation of bonding strength and of failure modes has been found in prior experiments, the influence of material variations on the forming and failure behavior (esp. the fracture pattern) is numerically studied. Finally, the capabilities of the model are demonstrated on a swivel bending process to form hat profiles.

Sandwich Manufacturing

To conduct material experiments on sandwich sheets, the utilized sheets are self-produced with lab-scale equipment by roll-bonding [8] with a 1.0242 (S250) zinc-coated metal sheet, the epoxy resin adhesive Köratac 201 FL, and a PP/PE copolymer foil, as described in [9]. Figure 1 gives a schematic overview of the process. First, the metal and polymer surfaces are cleaned with acetone to remove grease and other impurities affecting the bonding quality. Then, the epoxy adhesive is applied to the metal sheet with the help of a spiral scraper to distribute the adhesive evenly. Next, the adhesive is thermally activated for 3 min at 230 °C while the polymer is heated up to 120 °C. Finally, the sheet is bonded to the polymer foil by rolling the composite in a rolling mill. By rolling the metal sheet on the polymer, the bonding is continually created when the composite enters the rolling mill. This continuous process (instead of an immediate full contact) helps to avoid air inclusions and is suitable for industrial coil processing chains.

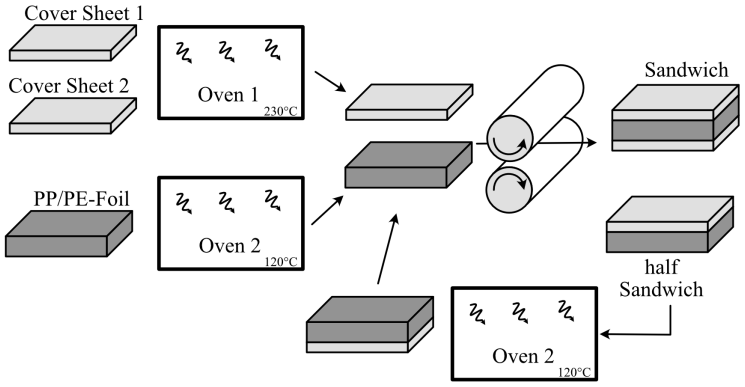

Fig. 1. Schematic roll-bonding process to manufacture metal-polymer-metal sandwich sheets.

Material Modeling

To develop a material model of the core materials reflecting their forming and failure behavior, standard-size and short-size tensile tests on the polymer foil and lap-shear tests on full metal-polymer sandwiches are conducted.

To gain flow curves of the utilized steel, standard tensile tests according to DIN EN ISO 6892-1 are performed on ten specimens, of which the resulting minimal, mean, and maximum flow curves are shown in Figure 2. The examined steel batch shows a significant variability in the flow curve, which is especially pronounced in the beginning of the plastic deformation up until ca. $\varepsilon = 6\%$. Additionally, it has to be noted that already the small temperature changes on the specimen's surface due to the heat generated by the plastic deformation can significantly influence the resulting flow curve [10]. However, since temperature effects are not studied in this work, the sandwich model is assumed to experience the same thermal conditions as the tensile test. The measured flow curve is applicable to the model because the flow curve will then incorporate the same temperature effects as occur in the forming process examined later. Similar thermal conditions can be assumed for forming processes with full-facial tool contact (e.g., swivel bending) since the generated heat will be dissipated

through the tool contact. The temperature rise in the sandwich sheet will therefore not be higher than in the tensile test.

For the polymer foil, a tensile test is conducted on a 25×180 mm strip specimen according to DIN EN ISO 527-3. Local strains (true strain) and strain rates are measured on the polymer foil in longitudinal φ_y $\dot{\varphi}_y$ and transversal φ_x, $\dot{\varphi}_x$ direction via digital image correlation with GOM Correlate 2022 of a pre-applied statistical gray scale pattern (see Figure 3). The strains are evaluated on 16 horizontal sections. For each section, the arithmetic mean of the strains is calculated. With regard to thermal effects, the same considerations apply to the polymer as to the steel [11]. When used in sandwich sheets, heat generated through plastic work will be immediately dissipated through the high thermal conductivity of the metal cover layer. Therefore, no high temperature change is expected in the studied quasi-static forming applications.

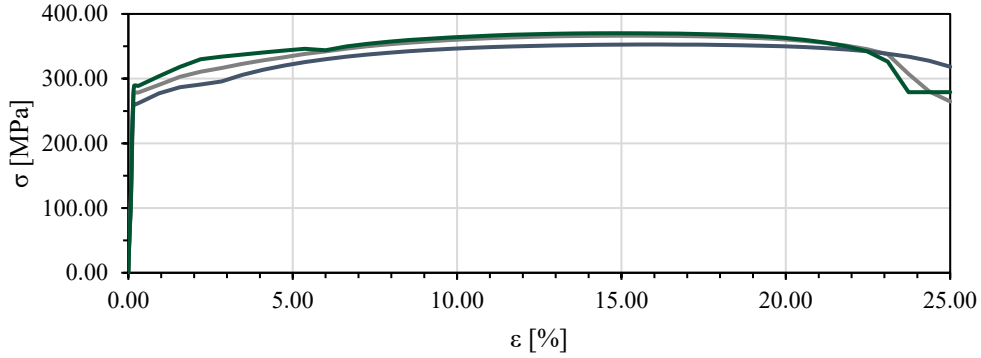

Fig. 2. Mean, minimum, and maximum results of ten tensile tests on the examined steel batch of 1.0242.

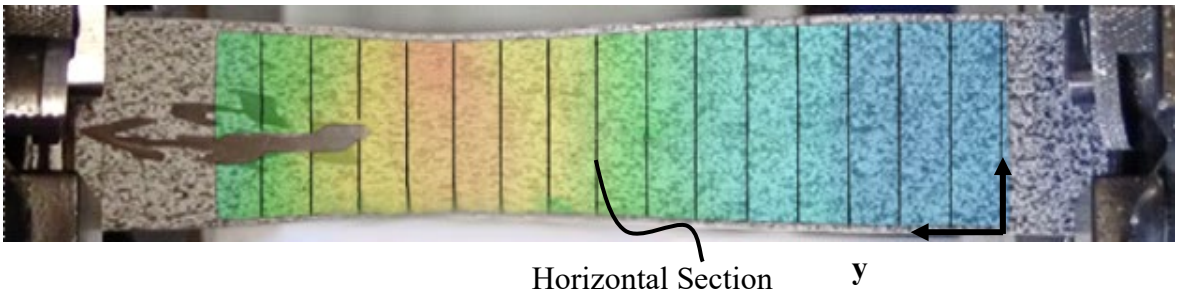

Fig. 3. Digital Image Correlation on the polymer foil and evaluation of the local strains at horizontal sections.

To derive the strain rate dependent plastic behavior of the polymer foil, first, Poisson's ratio for plastic deformation in the cross-section is calculated according to Equation 1 from the ratio of longitudinal to transversal strain.

$$\nu_y = -\frac{\varphi_y}{\varphi_x} \tag{1}$$

Assuming isotropic plastic behavior, true stresses are then derived from the force measurement by dividing by the cross-section

$$A_{xz} = A_{xz,0} e^{-2\nu_y \varphi_y}\,, \tag{2}$$

where $A_{xz,0}$ is the initial cross-section of the strip-specimen:

$$\sigma_y = \frac{F_y}{A_{xz}}. \tag{3}$$

The resulting flow surface in dependence on strain and strain rate is shown in Figure 4. From this flow surface, iso-strain flow curves (black lines in Figure 4) are derived from points of equal strain on the flow surface. The resulting iso-strain curves are depicted in Figure 5. The strongest strain rate

dependency is observed at low strain levels. At higher strain levels, the apparent strain rate dependency decreases.

To model the strain rate dependency in the examined load range, Cowper-Symonds's model (cf. Equation 4) is calibrated to the minimal iso-strain curve of the flow surface (cf. Figure 5a, highlighted in green).

$$\sigma = \sigma_{\text{stat}} \left(1 + \frac{\dot{\varphi}}{C}\right)^{P} \tag{4}$$

While a decreasing strain rate dependency at higher strains is not expected in typical material laws, a plausible explanation for the observed decrease is local temperature rise due to plastic work, which counteracts the strain rate hardening. This effect is expected to be strongest in regions of high deformation and, therefore, high strain.

Therefore, the minimal iso-strain curve is chosen for the calibration of Cowper-Symonds' model, since it reflects best the pure strain rate dependency (without temperature influence) and since it covers the broadest strain rate region. Even though this may lead to an overestimated strain rate hardening at high strain levels (when temperature weakening is not considered), this approach may be used here, since the model is only used for quasi-static forming applications with limited heat generation, easily dissipated through the metal cover layers. Furthermore, valid predictions of the model are limited to applications within the examined strain rates (from ca. $10^{-6}s^{-1}$ to $5 \cdot 10^{-6}s^{-1}$ in this example).

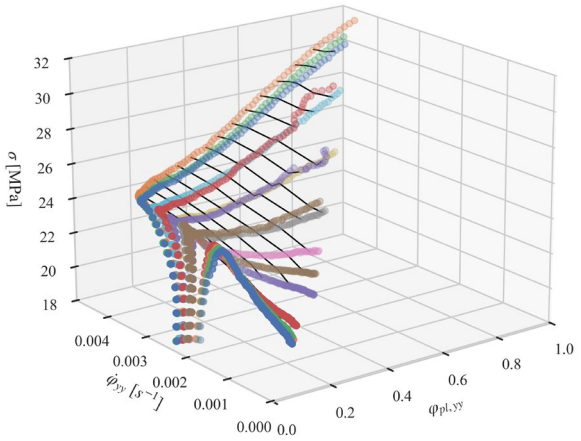

Fig. 4. Flow surface over strain and strain rate derived from the experiment. Some iso-strain curves are shown as black lines.

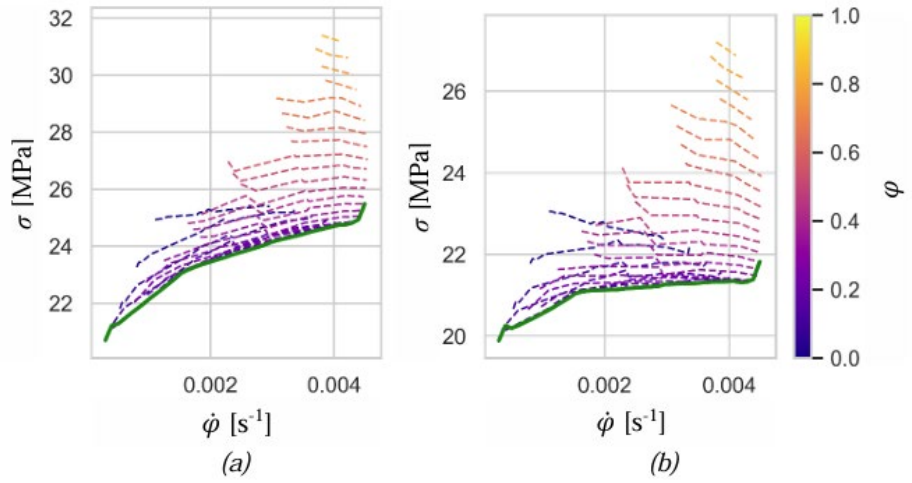

Fig. 5. Iso-strain flow curves of the polymer foil before (a) and after (b) strain rate compensation. Compensation was done with Cowper-Symonds-Model on the minimal iso-strain curve (highlighted in green).

Due to the strong work-hardening effect of the polymer foil, plastically deformed areas of the polymer get stabilized, and the necking wanders over the specimen. As a result, a “shoulder” formation is observed on the specimen, and no material failure occurs in the standard-size tensile test.

Therefore, to model material failure, short tensile tests are used. Slits of 5 mm are milled into the metal layer of half-sandwich specimens (metal-polymer sandwich, missing the second metal layer) to free the polymer, which ensures rupture happens in the test while providing enough undeformed area to track the elongation with a video system (cf. Figure 6, where deformation only takes place between the two red lines).

Fig. 6. Short tensile test specimen. Deformation only takes place between the two red bars. The specimen elongation is tracked with a video system on the undeformed gray pattern.

Material damage and resulting failure are accounted for in the material model with a damage function $D(\varphi_{\mathrm{pl}})$ that weakens the flow stress according to eq. 5 and ultimately leads to rupture for $D = 1$.

$$\sigma_{\mathrm{eff}} = \sigma\left(1 - D\left(\varphi_{\mathrm{pl}}\right)\right) \tag{5}$$

As a damage evolution function, a customizable two-parameter exponential function is chosen with φ_{fail}, the plastic strain at rupture, and the parameter n, which allows adjusting the evolution from an early damage logarithmic ($n < 0.73$) to an exponential increasing characteristic ($n > 0.73$) with $n \approx 0.73$ resembling a linear development.

$$D\left(\varphi_{pl}\right) = \left(\frac{e^{\varphi_{pl}} - 1}{e^{\varphi_{\mathrm{fail}}} - 1}\right)^{n} \tag{6}$$

Values for φ_{fail} and n are obtained by numerical calibration with LS-OPT of an FE simulation to the experimental data until sufficient adherence is achieved. An example of resulting material parameters that are used in the following to model the polymer foil in LS-DYNA with the MAT_SAMP_1 model is listed in Table 3 in the appendix. It has to be noted that due to the single-specimen approach in this work, the provided data does not represent a statistically proven dataset. Therefore, quantification of the scatter in the material itself and possible error due to the characterization method cannot be given.

The focus of this work is to present a characterization concept. However, since the experimental setup relies on standard, widely validated equipment, significant deviations of the results will mainly arise from the specimen itself. Comparison with literature data on the same polymer foil shows that the derived flow curve lies in the same order of magnitude [4]. The principal mechanical behavior of the polymer foil is captured well with the proposed model.

Modeling of the adhesive is based on the results of lap-shear tests [12] of metal-metal sandwich specimens with a 5 mm overlap and a total specimen length of 215 mm. To model the adhesive, LS-

DYNA's MAT_COHESIVE_MIXED_MODE model is used, which uses a bilinear traction-separation law for shear (tangential) and tensile (normal) load [13], [14]. The corresponding material parameters, the peak tractions S, T from which delamination starts, and the energy release rates $GIC, GIIC$, which describe the total area under the traction-separation curve, are again calibrated numerically with LS-OPT. The resulting parameters are listed in Table 4 in the appendix.

Numerically finding good estimates for the stiffness E was found to be difficult. However, since a very stiff force displacement response was observed in the experimental lap-shear test, a stiffness similar to that of the steel was chosen. The stiffness is defined as the stress per unit length and models the elastic stress response to a length change of the cohesive element. Therefore, it is independent of the element's thickness. However, the peak tractions and the energy release rates depend on the element size, and adaptation to different meshes would be needed, consequently. Nevertheless, since in this work the same mesh sizes are used for both the calibration and the subsequent forming applications, there is no necessity to adapt the material parameters.

Model Validating

To validate the sandwich interface and core model, FEM simulations of swivel bending tests are compared to their corresponding experimental results. According to the foreseen use of the sandwich sheets for double-hat crash absorbers, strip specimens of a half hat-profile, formed with two consecutive 90° bends, are examined (cf. Figure 7). To capture the properties of the core and interface material, springback and the displacements between the outer and inner metal sheets in the direction of the neutral axis are measured.

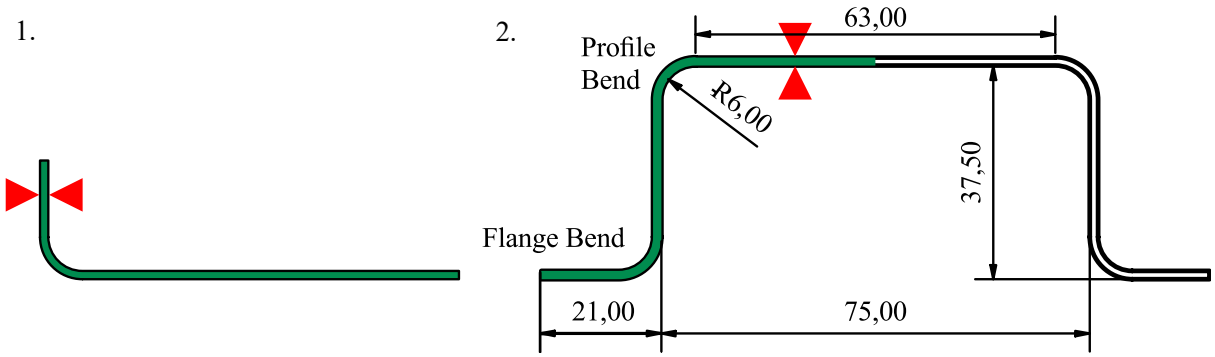

Fig. 7. Bending sequence of the hat profile. Triangles mark the fixed support. Strip specimen highlighted in green.

For the displacement measurement, the method proposed by [15] and improved by [10] is employed: before bending the sandwich specimen, the cross-section is ground to achieve an even and scratch-free surface. Then, transversal marks are pressed into the surface at equal distances. After bending the specimen, the displacements between every two corresponding marks in the outer and inner metal layers can be measured with a microscope using a 100x magnification and applying tile stitching with automatic depth focus adjustment (cf. Figure 8).

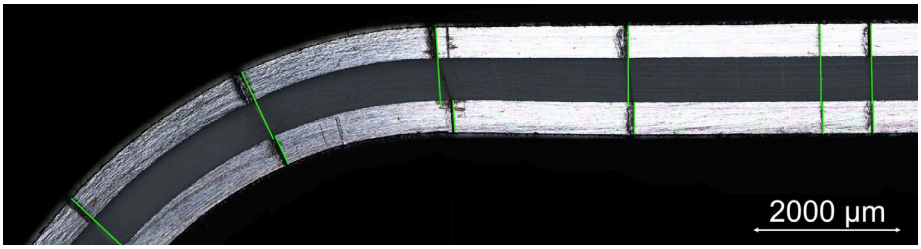

Fig. 8. Cutout of the flange bend of the sandwich specimen with displacement marks (green highlights used to measure the displacement).

The FE model of the bending tests to be validated is built up with solid elements of 0.25 mm length in the longitudinal direction and 2 mm in the transverse direction. Over the thickness, three elements

are used for the metal and polymer layers, while one element is used for the adhesive (cf. Figure 9). A 6 mm radius and a constant bending speed $\dot{\varphi}$ of 9°/s are used for the swivel bending process. The bending process is simulated in a two-step approach considering springback: first, the flange bend and the occurring springback are simulated. Then, the resulting geometry, as well as residual stresses and plastic strains are transferred to a second model to bend the side wall, again under consideration of the springback. The metal layer displacements are extracted from the innermost node line of the metal layer outer edges of the resulting geometry and are evaluated with a Python script for comparison with the experimental results.

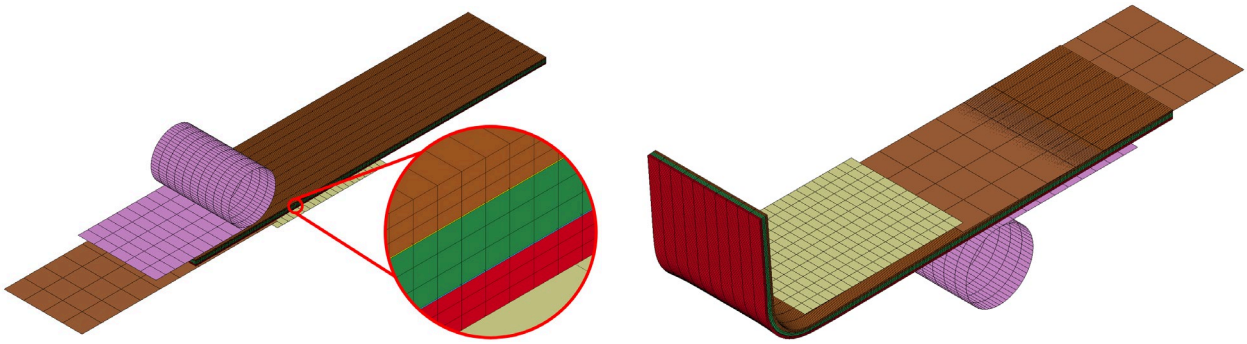

Fig. 9. Finite element model of the two consecutive swivel bending steps.

To validate the developed material model, the results from the experimental bending tests and the corresponding FEM simulations are compared. First, Table 1 compares the profile angles after springback at the flange bend and at the profile bend. The results prove that the simulation in principle matches the experimental results, despite a mismatch of ca. 1°. Furthermore, to estimate the influence of the DIC-based strain rate reconstruction, perturbations of the strain rate dependent stress model were assessed. Variations of ± 2 % resulted in less than 1.5° variation in springback.

Noticeable is the differing trend in the simulation compared to the experiment: While in the experiment the first bend angle (flange angle) is greater than the second angle (profile angle), in the simulation the angles are vice versa. When interpreting the results, one has to consider that due to the sequential bending process, deviations and errors are added up. Thus, every deviation in the first bending step directly influences the results of the second step. Therefore, the opposite trend of the bend angle in the simulation could be explained by the superposition of the general simulation error and the error propagation from the first bending step.

Table 1. Hat-profile angles after springback (measured at enclosing sheet).

Position	Experiment	Simulation
Flange	94.5°	93.6°
Profile	93.5°	94.5°

A more detailed validation of the polymer and the adhesive model is possible with the comparison of the cover layer displacements. Since the cover layers are purely elastically loaded, the displacements depend solely on the interface and polymer properties (when assuming an equal elastic modulus for all relevant cover sheets). To distinguish the direction of displacement, a sign convention is introduced: displacements of the upper layer to the lower layer in the positive coordinate direction are accounted for as positive, while in the opposite case they are accounted for as negative (cf. Figure 10). The bend line coordinate x is defined to start in the center of the hat profile, thus at the long side of the strip specimen, and proceeds from there to the outer edge (cf. Figure 10).

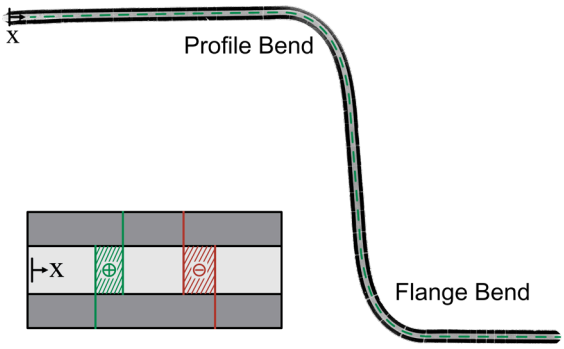

Fig. 10. Definition of the bend line coordinate and sign convention for the evaluation of the cover layer displacements.

The resulting cover layer displacements δ are shown in Figure 11. The general development of the displacements matches well in experiment and simulation. Due to the swivel bending process, the displacements fall fast to nearly zero at the free edges, which were clamped during bending. In the bending zones, a positive displacement peak is followed by a negative peak for a right bend. The displacements cross zero near the midpoint of the bend and reach their limits (maxima/minima) near the end of the bending regions, which aligns with the findings reported for V-bending reported in the literature [10]. In the side wall between the two bends, the displacements overlap, wherefore they do not fall to zero in the experiment as well as in the simulation. Here again applies the error propagation stated for the springback angle. While the first bend in the simulation still matches the experimental results very well, a greater discrepancy is found in the second bend. Nevertheless, since the principal forming behavior is reflected well, the material model is considered to be valid.

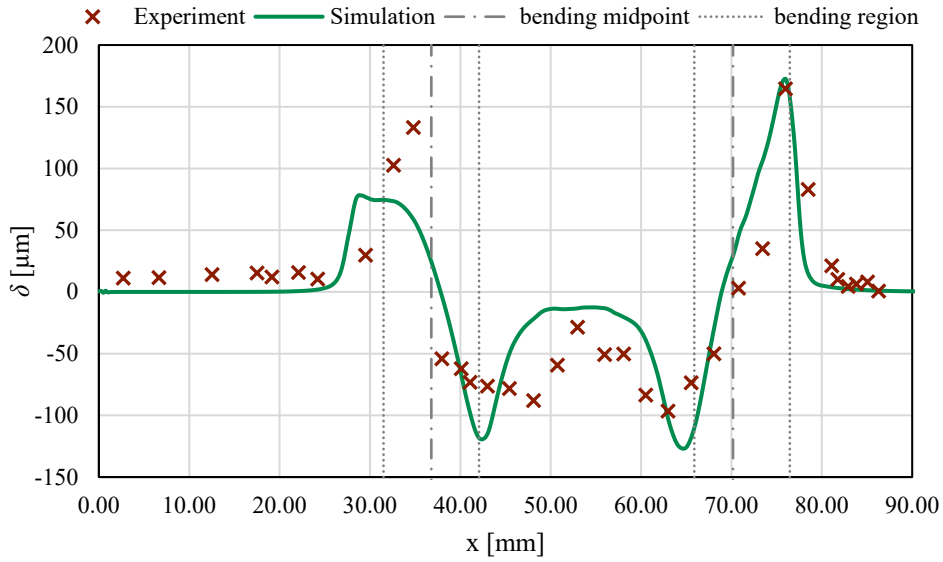

Fig. 11. Cover layer displacements in experiment and simulation.

Parameter Study on the Influence of Material Variabilities

To study the effect of inherent material variabilities on the forming and failure behavior, a full factorial parameter sweep of small changes in the material strengths is conducted, and their effect on the failure mode of lap-shear tests is analyzed. While for the metal sheets, enough tensile tests were conducted to derive a minimum and maximum flow curve, not enough results were available for the polymer and the adhesive to capture the statistical distribution of their properties. Therefore, changes of $\pm 10\%$ in the nominal strengths (flow curves and peak traction, respectively) are assumed. This assumption is validated on simplified material tests. Tensile tests of three polymer specimens without capturing the local strains yield a variance of 0.4% to 2.8% of the yield stress, while the variance of

the peak stress of eight full sandwich lap-shear tests is 7.9% of the nominal value. Consequently, the ±10% assumption is a realistic assumption for the adhesive and conservative for the polymer foil, taking into account that the shear behavior (which is unknown from the tensile test) might differ significantly from the tensile strength. However, this does not represent a statistically derived process distribution but rather a structured sensitivity range to evaluate failure mode transitions.

The FE model of the lap-shear tests is presented in Figure 12 and uses the same element sizes as the bending model. The perturbed material parameter curves are compiled in Figure 13.

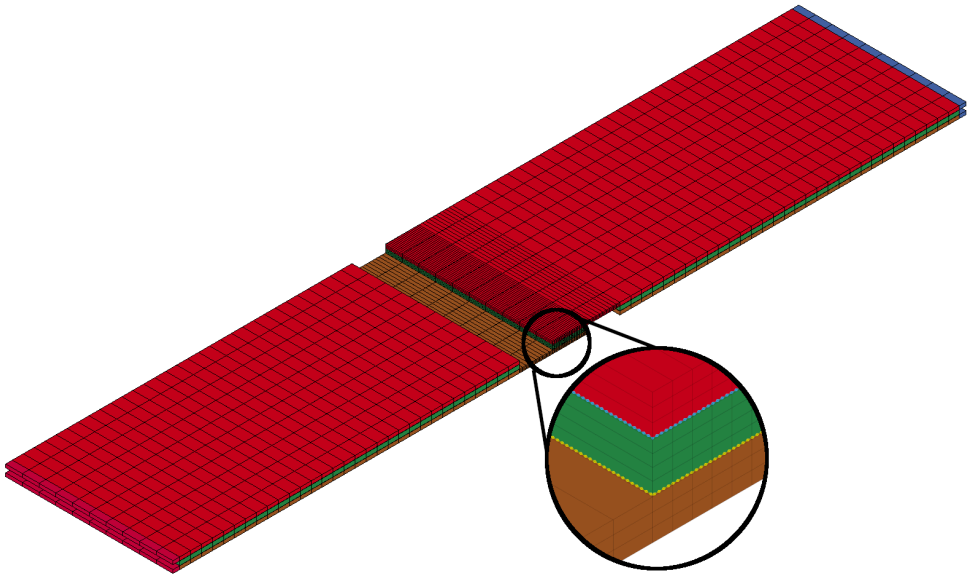

Fig. 12. FE model of the lap-shear test.

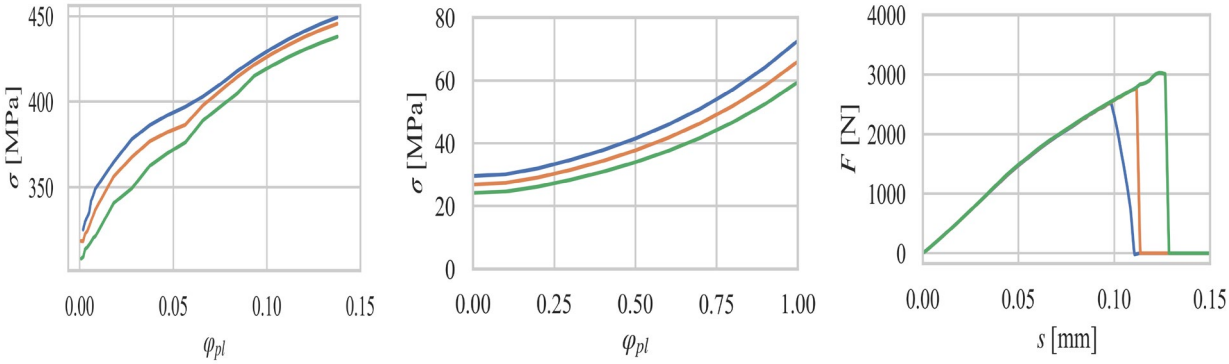

Metal Polymer Adhesive

Fig. 13. Perturbed material curves (minimal, nominal, and maximal strength) for the parameter study.

The results of the parameter study are shown in Figure 14. The occurring failure modes can be divided into three groups: (1) a long-stretched polymer in the case of reduced polymer and increased adhesive strength, (2) an S-shaped bend of the polymer foil mixed with delamination of the adhesive for equally directed changes of polymer and adhesive strength, and (3) fracture of the polymer as the main failure criteria for simulations with increased polymer strength and decreased adhesion. In all three groups, the influence of the steel strength is negligible, since the plastic deformation of the cover layers is rather limited. The small effects occurring in relation to a steel strength change more probably result from numerical effects.

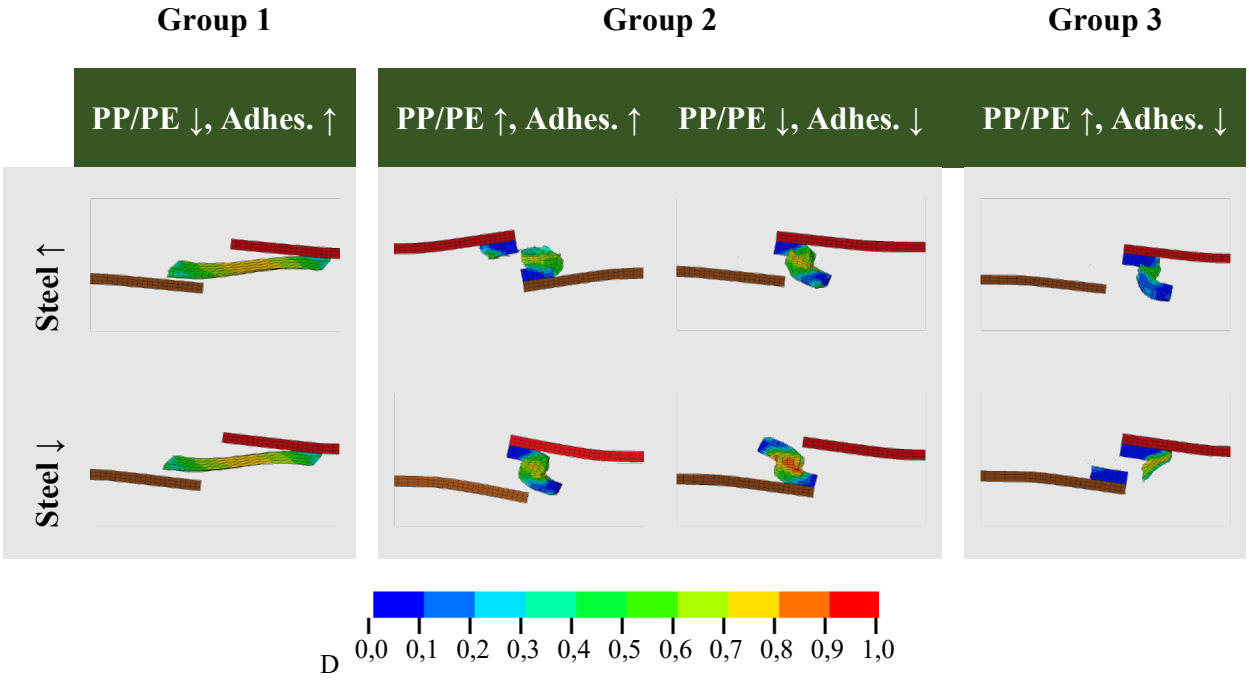

Fig. 14. Resulting failure modes and polymer damage in simulated lap-shear tests. The material strength parameters were varied in a full factorial approach.

It has to be noted that in the first failure mode in group 3 (PP/PE ↑, Adhes. ↓, Steel ↑), the fracture of the polymer happens first. The subsequent delamination only occurs due to numerical issues with the failed polymer. Thus, the failure principle lies nevertheless in the polymer fracture. This becomes clear when the shape is compared with the results of group 2, where no polymer elements were deleted.

A comparison of the simulated failure modes to experimental lap-shear results of several material combinations (cf. Figure 15) shows that the simulation is capable of reflecting various failure modes that occur in reality. Additionally, the parameter study reveals that the factual failure mode mainly depends on a complex balance of polymer and adhesive strength. Small perturbations can result in a different mode. This indicates that the examined polymer-adhesive combination is at the transition point between adhesive and cohesive failure, as has also been observed for a similar combination in the literature [6], [7]. Since the forming behavior ultimately accumulates to the examined failure modes in the lap shear tests, the inhomogeneous material behavior can be simulated well with the proposed model in forming and failure studies.

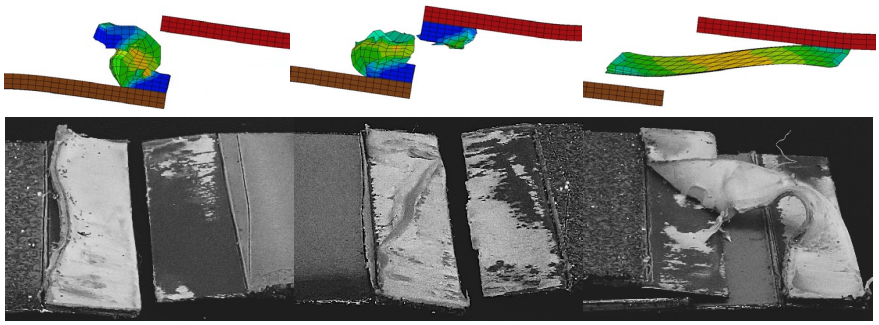

Fig. 15. Comparison of simulated (top) and experimental (bottom) lap-shear test failure modes.

Predicting Springback and Material Failure in the Profile-Bending Process

In contrast to conventional three-layer models, which do not consider the adhesive, the developed and validated model of the sandwich materials can be used in forming process simulations to predict springback and possible material failure. While a three-layer approach yields results as shown in

Figure 16 with significant edge displacement and a mismatch of the predicted angle after springback (95.7° for the model without consideration of the bonding), the presented modelling approach incorporating the adhesive is capable of accurately predicting springback and edge displacement (cf. Table 1 and Figure 11).

Furthermore, the model can be used to study the influence of first, the inherent variation of the adhesive strength of a stable sandwich manufacturing process on the forming process, and secondly, the effect of outliers in the bonding quality (e.g., through local bonding defects, low manufacturing quality, etc.) on the forming behavior.

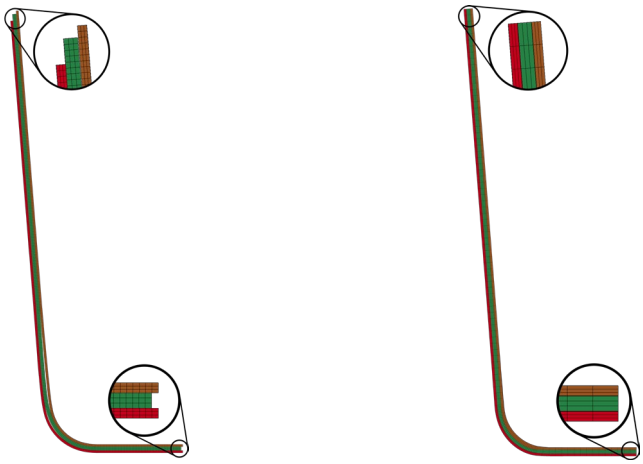

(a) without adhesive *(b) with adhesive*

Fig. 16. Bending simulation of a three-layer specimen without adhesive compared to a simulation with adhesive.

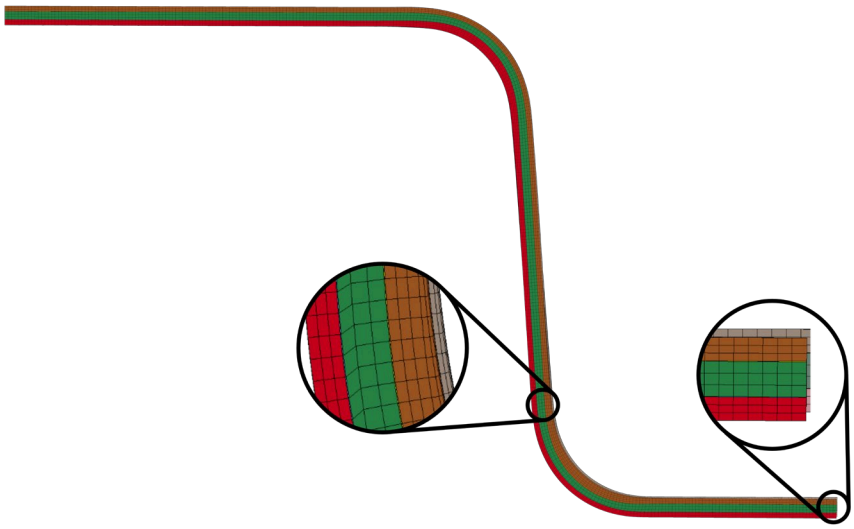

Fig. 17. Geometric deviation between simulated bending specimens with maximal adhesive (grey) and minimal adhesive (colored) strength.

Table 2. Simulated springback of the maximal and minimal adhesive strength variation compared to the nominal springback angle.

Position	Maximal variation	Nominal	Minimal variation
Flange	93.9°	93.6	94.1°
Profile	94.1°	94.5	93.9°

The profile angles vary after the springback only in a small range, from 93.6° to 94.1° for the flange and from 93.9° to 94.5° for the profile bend. Therefore, it can be concluded that the process inherent variation of the adhesive strength of good quality sandwich sheets has a negligible influence on the geometric accuracy of the hat profiles.

However, a greater impact of the adhesive strength is seen in low-quality bondings. Figure 18 shows, for example, delamination and the consequent buckling of a profile bend with significantly lower adhesion strength, as it can occur for sandwich sheets with defective or partially defective bonding. By considering the weakened adhesive (reduction to ca. 11 % of the nominal strength) in the simulation, the same failure mode as observed in bending experiments is predicted.

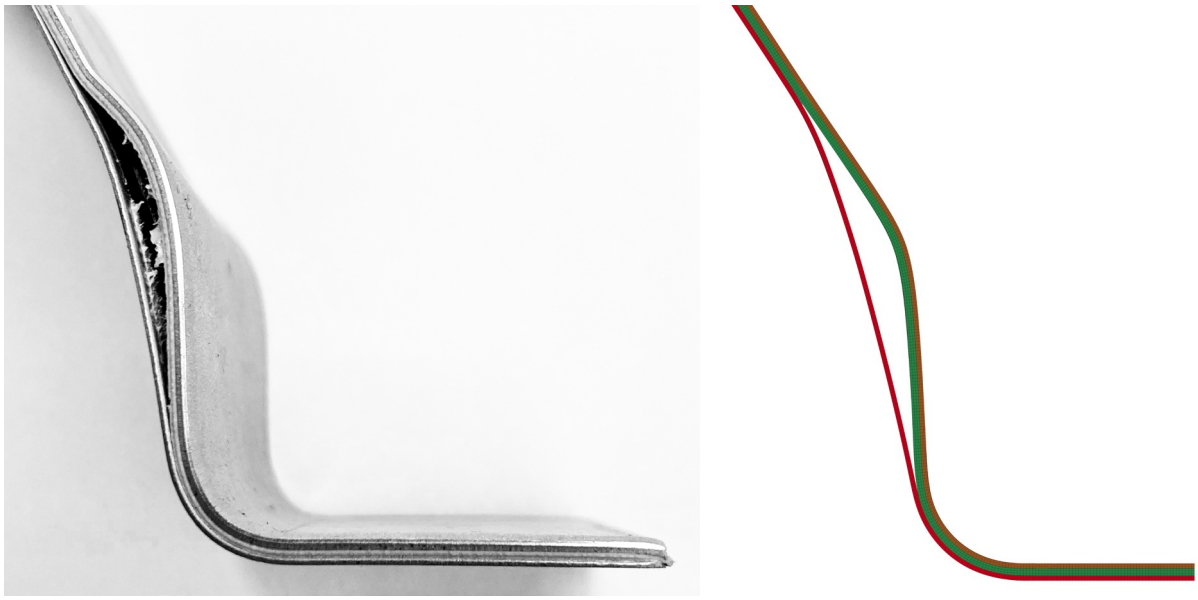

(a) experiment *(b) simulation*

Fig. 18. Delamination and resulting buckling in the bending process due to low bonding quality in the experiment and simulation.

Conclusion

This work presents an approach for deriving a strain rate-dependent polymer model for FEM simulations of the forming and failure behavior of metal-polymer-metal sandwich sheets. Springback and cover layer displacements can be predicted using the FE model and are used to validate the proposed approach with experimental results.

The parameter study on the influence of material inhomogeneities shows that the failure mode of mpm-sandwiches can vary significantly by small changes in the balance of steel, polymer, and adhesion strength. By respecting the parameter deviations in FEM simulations, experimental failure modes can be reproduced.

The developed sandwich material model has been proven to be usable in bending process simulations. It is thus possible to more accurately predict the sandwich's forming behavior in a profile manufacturing process, which helps tune the sandwich and forming process parameters. Study of the model's applicability to other forming processes is subject to future research. Furthermore, improving the material models to reflect a greater range of strain rates and incorporating temperature effects are further research directions to facilitate consistent simulation of the forming as well as the crash performance of sandwich sheets.

Appendix

Table 3. Summary of material parameters for the MAT_SAMP_1 polymer model.

ρ	E	ν_{el}	ν_{pl}	φ_{fail}	Flow and Damage Curves							
					$\dot{\varphi}$	σ [MPa]						
					$10^{-6}\,\frac{1}{s}$	26.9	31.5	37.7	66.0	151	377	838
					$10^{-3}\,\frac{1}{s}$	30.3	35.6	42.6	74.5	170	426	945
0.957 g cm^{-3}	1024 MPa	0.4	0.26	2.7	$10^{-2}\,\frac{1}{s}$	32.8	38.5	46.1	80.6	184	461	1023
					$10^{-1}\,\frac{1}{s}$	36.6	42.9	51.4	89.9	205	514	1141
					$1\,\frac{1}{s}$	42.3	50.0	59.4	104	237	595	1320
					$D(\varphi)$	0.0	0.33	0.44	0.61	0.74	0.87	1.0
					φ_{pl}	0.0	0.3	0.5	1.0	1.6	2.2	2.7

Table 4. Material parameters for the MAT_COHESIVE_MIXED_MODE adhesive model.

	Mode I	Mode II
E	$210\,\frac{\text{GPa}}{\text{mm}}$	$210\,\frac{\text{GPa}}{\text{mm}}$
G^c	$0.65\,\frac{\text{mJ}}{\text{mm}^2}$	$0.88\,\frac{\text{mJ}}{\text{mm}^2}$
T, S	68.15 MPa	22.95 MPa

Acknowledgement

This research was funded by the Deutsche Forschungsgemeinschaft (DFG, German Research Foundation) – 523138878.

References

[1] H. Palkowski and A. Carradò, "Metal-Polymer-Metal Laminates for Lightweight Application," *Key Eng. Mater.*, vol. 684, pp. 323–334, Feb. 2016, doi: 10.4028/www.scientific.net/KEM.684.323.

[2] I. Burchitz, R. Boesenkool, S. van der Zwaag, and M. Tassoul, "Highlights of designing with Hylite – a new material concept," *Mater. Des.*, vol. 26, no. 4, pp. 271–279, Jun. 2005, doi: 10.1016/j.matdes.2004.06.021.

[3] Sanjeev Sharma, "Sandwich Steels for Crash Energy Absorption Applications," Dissertation, University of Warwick, 2014. Accessed: Feb. 13, 2025. [Online]. Available: https://wrap.warwick.ac.uk/id/eprint/74157/1/WRAP_THESIS_Sharma_2014.pdf.

[4] M. Harhash, M. Kuhtz, J. Richter, A. Hornig, M. Gude, and H. Palkowski, "Trigger geometry influencing the failure modes in steel/polymer/steel sandwich crashboxes: Experimental and numerical evaluation," *Compos. Struct.*, vol. 262, p. 113619, Apr. 2021, doi: 10.1016/j.compstruct.2021.113619.

[5] V. Harms, M. Harhash, A. Carrado, and H. Palkowski, “Energy Absorption Behavior of Metal/Polymer/Metal Sandwich Crash Structures,” *Key Eng. Mater.*, vol. 746, pp. 275–281, Jul. 2017, doi: 10.4028/www.scientific.net/KEM.746.275.

[6] M. Harhash, M. Kuhtz, J. Richter, A. Hornig, M. Gude, and H. Palkowski, “Influence of Adhesion Properties on the Crash Behavior of Steel/Polymer/Steel Sandwich Crashboxes: An Experimental Study,” *Metals*, vol. 11, no. 9, p. 1400, Sep. 2021, doi: 10.3390/met11091400.

[7] J. Richter, M. Kuhtz, A. Hornig, M. Harhash, H. Palkowski, and M. Gude, “A Mixed Numerical-Experimental Method to Characterize Metal-Polymer Interfaces for Crash Applications,” *Metals*, vol. 11, no. 5, p. 818, May 2021, doi: 10.3390/met11050818.

[8] H. Palkowski, P. Giese, V. Wesling, G. Lange, S. Spieler, and J. Göllner, “Neuartige Sandwichverbunde – Herstellung, Umformverhalten, Fügen und Korrosionsverhalten,” *Mater. Werkst.*, vol. 37, no. 7, pp. 605–612, Jul. 2006, doi: 10.1002/mawe.200600039.

[9] O. Sokolova, A. Carradó, and H. Palkowski, “Production of Customized High-Strength Hybrid Sandwich Structures,” *Adv. Mater. Res.*, vol. 137, pp. 81–128, Oct. 2010, doi: 10.4028/www.scientific.net/AMR.137.81.

[10] J. Buhl, “Umformverhalten und Grenzen von Schichtverbundwerkstoffen,” Shaker Verlag GmbH, DE, 2014. Accessed: Dec. 17, 2025. [Online]. Available: https://doi.org/10.2370/9783844028225.

[11] P. Eyerer, “Eigenschaften von Kunststoffen in Bauteilen,” in *Polymer Engineering 1*, P. Eyerer and H. Schüle, Eds., Berlin, Heidelberg: Springer Berlin Heidelberg, 2020, pp. 89–519. doi: 10.1007/978-3-662-59837-5_3.

[12] Normenausschuss Materialprüfung, *Klebstoffe - Bestimmung der Zugscherfestigkeit von Überlappungsklebungen*, DIN EN 1465, Jul. 2009. doi: 10.31030/1507601.

[13] B. Engel, J. Buhl, and C. Heftrich, “Modelling and Optimization of Lightweight-Sandwich-Sheets with an Adhesive Interlayer for the Forming Process Die Bending,” *Procedia CIRP*, vol. 18, pp. 168–173, 2014, doi: 10.1016/j.procir.2014.06.126.

[14] Ansys Inc., *Volume II – Material Models*, 15th ed. in LS-DYNA Keyword User’s Manual. 2024. Accessed: Feb. 01, 2025. [Online]. Available: https://lsdyna.ansys.com/manuals/.

[15] L. Keßler, *Simulation der Umformung organisch beschichteter Feinbleche und Verbundwerkstoffe mit der FEM*. Shaker, 1997.